**Philippine Journal of Science**
152 (4): 1371-1386, August 2023
ISSN 0031 - 7683
Date Received: 31 Jan 2023

# Development of Risk-targeted Seismic Hazard Maps for Low-rise and Mid-rise Reinforced Concrete Buildings in the Philippines

**Royce Argel N. Mallari[1]*, Lessandro Estelito O. Garciano[1], and Henremagne C. Peñarubia[2]**

[1]Department of Civil Engineering, De La Salle University, Manila City, National Capital Region 1004 Philippines
[2]Philippine Institute of Volcanology and Seismology, Department of Science and Technology Philippines, Quezon City, National Capital Region 1101 Philippines

**The seismic hazard maps of the Philippines provide spectral acceleration mean values that describe the probability of occurrence of area-specific ground motion hazards due to earthquakes in the country. However other countries have progressed from developing hazard maps to risk-targeted maps that include information on the probability of collapse of buildings. This is the research gap that this study aims to bridge and, thus, developed maps of risk-targeted ground motions (RTGM) for the Philippines using the City of Manila as the area of focus. The maps will be created using the procedure suggested in ASCE 7-16 in obtaining the risk-targeted maximum considered earthquake ($MCE_R$). The probabilistic $MCE_R$ will be created using the information obtained from the seismic hazard and the generic fragility curve that will represent the performance of buildings during a maximum considered earthquake (MCE) event. In this study, the seismic hazards were obtained using the same procedure, decision-making, and empirical formula as the one used in developing the Spectral Acceleration Maps of the Philippines (SAM PH). While the generic fragility curve was described by a function with a lognormal standard deviation, β, of 0.7. With a considered risk level of 1% probability of collapse in 50 yr, the developed RTGM maps are presented in this study. In the analysis of results, the probabilistic $MCE_R$ is lesser than the MCE level spectral accelerations in the majority of the area in Manila due to the influence of the building's collapse capacity for stiff soil profiles. The opposite can be seen in softer soil profiles. However, the final $MCE_R$ values are slightly larger than the MCE values due to the application of the directivity factors.**

Keywords: DSHA, MCE, $MCE_R$, PSHA, RTGM

## INTRODUCTION

The National Structural Code of the Philippines 2015 (NSCP 2015), the latest seismic design procedure in the Philippines, is based on the seismic provisions of the 1997 Uniform Building Code (UBC 1997), which utilizes ground motion values with a 10% probability of exceedance in 50 yr or 475 yr return period (ASEP 2015). To enhance the latest seismic design procedure stated in NSCP 2015, the Philippine Institute of Volcanology and Seismology of the Department of Science and Technology (DOST-PHIVOLCS) released the Philippine Earthquake Model (PEM) on 17 Jan 2018 (DOST-PHIVOLCS 2017). The PEM is the first generation uniform seismic

*Corresponding author: ranmallari07@gmail.com

hazard map for the Philippines that was developed by the DOST-PHIVOLCS in technical consultation with the Department of Public Works and Highways, National Housing Authority, Office of Civil Defense, Metro Manila Development Authority, Philippine Institute of Civil Engineers, Association of Structural Engineers of the Philippines (ASEP), De La Salle University, University of the Philippines Diliman–Institute of Civil Engineering, Philippine Insurers and Reinsurers Association of the Philippines (PIRA), and the local governments in the National Capital Region using the probabilistic seismic hazard assessment (PSHA) methodology. It provides maps showing peak ground acceleration (PGA) and spectral acceleration ($S_a$) values for different periods based on seismic hazards with a 10% probability of exceedance in 50 yr.

With the improvements and latest developments in seismic hazard assessment, and in technical collaboration with the Global Earthquake Model (GEM) Foundation, Geoscience Australia, and the ProjectSAM Committee of the ASEP, the DOST-PHIVOLCS developed and published the Spectral Acceleration Maps of the Philippines Atlas (SAM PH 2021) on 23 Mar 2021 (DOST-PHIVOLCS 2021). SAM PH 2021 provides spectral acceleration values based on the maximum considered earthquake (MCE) or ground motion values with a 2% probability of exceedance in 50 yr. The SAM PH 2021 was leveraged upon the DOST-PHIVOLCS GEM Foundation technical paper collaboration (Peñarubia *et al.* 2020) and is planned to be adopted in the next edition of the NSCP.

However, these hazard maps only provide uniform hazards that are described by the earthquake's probability of recurrence and not by the structure's probability of collapse. The United States (US) led in the development of risk-targeted ground motion (RTGM) maps in the country by following the works of Luco and co-authors (2007) by introducing the concept of the risk-targeted maximum considered earthquake ($MCE_R$) that are ground motions that will produce a uniform risk of collapse of 1% in 50 yr ($2 \times 10^{-4}$). The RTGM was obtained by integrating a generic fragility curve that is described by a lognormal standard deviation, β, equal to 0.8 that then later on reduced to 0.6 in ASCE 7–10. Douglas and co-author (2013) find that a β value of 0.8 is too high and estimated that a β value of 0.5 is reasonable. Using the estimated β and a lower risk target of $1.0 \times 10^{-5}$ annual probability of collapse, they developed the RTGM maps for France. Silva and co-authors (2016) developed the RTGM maps for Europe using the Seismic Hazard Harmonization in Europe results for the seismic hazard with their estimated annual risk of collapse of $5.0 \times 10^{-5}$ and β = 0.6. These studies were used as the foundation and/or reference for the methodology and parameters used in creating RTGM maps in Romania (Vacareanu *et al.* 2018), Indonesia (Sengara *et al.* 2020), Iran (Taherian and Kalantari 2019), and Spain (Kharazian *et al.* 2021). Gkimprixis and co-authors (2019) conducted a review comparing the existing methodologies in developing risk-targeted seismic hazard maps. They also investigated the effectiveness of the current risk-targeting procedures applied in the US, wherein they found that aside from developing the risk-targeted seismic hazard maps, modification on the response modification factor, R, should also be analyzed. They also developed risk-targeted seismic hazard maps for Europe using risk-targeted behavior factors (RTBF) and a target of 1% probability of collapse in 50 yr. Due to such development, Douglas and co-authors (2019) applied the RTBF approach in generating risk-targeted maps for Italy.

To the best of the authors' knowledge, there are no publicly published seismic hazard maps in the Philippines that provide information on ground motions that gives a uniform risk of collapse to buildings at the time of this writing. Thus, it is necessary to improve the standards for the seismic design of structures in the country. This study's primary objective is to develop risk-targeted hazard maps for low-rise and mid-rise reinforced concrete (RC) buildings using the City of Manila as the main area of study. Subsequently, the lognormal standard deviation, β, used to define the generic fragility function that will represent the aforementioned buildings' collapse capacity will be determined in this study. In addition, the effects on the ground motion values when the collapse capacity of the buildings is integrated into the ground motion hazard will be investigated.

The RTGM maps developed in this study, if considered in low- and mid-rise RC building design, will provide a uniform risk assessment that may reduce the possibility of collapse during an MCE earthquake, whereas the methodology can be replicated to generate the RTGM maps for buildings in other areas of the Philippines.

## METHODOLOGY

### Geographical Information System (GIS) Mapping

The first part of the methodology is obtaining the stations where the seismic hazards will be assessed. This was achieved by mapping the City of Manila and dividing it using 2 km x 2 km grid lines, as shown in Appendix I. The intersection of the gridlines (referred to as grid points) will serve as reference locations for obtaining the seismic hazards. Additionally, the GIS map resulting from this process will serve as the basic framework for mapping the RTGM results.

**Probabilistic Seismic Hazard Assessment (PSHA)**

The PSHA of Manila was conducted to obtain the probabilistic hazard curves for each grid point established in the GIS map, as well as for each of the soil profile types listed in Appendix II. Additionally, the data, parameters, empirical models, and decision-making in creating SAM PH 2021 were used in this study for consistency. The complete discussion of the PSHA for the Philippines is discussed in the paper of Peñarubia and co-authors (2020). The resulting hazard curves will serve as the basis for determining the spectral accelerations that correspond to ground motions with a 2% probability of exceedance in 50 yr, which then will be used to design the building samples. Additionally, the hazard curves will also be used to calculate the probabilistic RTGM, which will be discussed in the succeeding sections. Appendix III shows examples of the hazard curve of one of the grid points (latitude: 14.63901, longitude: 120.94143) obtained from the PSHA of every soil profile type. $S_S$ and $S_1$ are spectral acceleration values for structure periods T = 0.2 s and T = 1.0 s, respectively.

**Building Samples**

Building samples are needed to generate the generic fragility function that will represent the collapse capacity of the buildings in Manila. Unfortunately, there are no available building stock data in the Philippines. Hence, the researchers decided to create 12 building samples following the logic tree in Appendix IV as a guideline. The logic tree ensures that the effects of [1] the building height based on the number of stories, [2] the rigidity and flexibility of structures based on height-to-width ratio, [3] the seismic demand that the structure will resist based on the structure's location from an active fault, and [4] the importance category of the structure and the soil condition at the site will be considered in the design of the building samples.

For the purpose of the study, the researchers also established that buildings with 1–3 stories will be classified as low-rise buildings, whereas buildings with 4–7 stories will be classified as mid-rise buildings as there is no standard classification of buildings based on their height or number of stories. For simplicity of modeling, building samples will have regular geometry with a fixed width of 6.0 m for each bay and a fixed inter-story height of 3.0 m. This simplification was based on the assumption that building samples must have an increment of at least 3.0 m in height and 6.0 m in length to have a significant impact on the lognormal standard deviation, β, which is used to define the generic fragility function.

Since the majority of the low-rise and mid-rise buildings in Manila are composed of RC frames, the building samples will be designed to have RC special moment frames using the ultimate and serviceability requirements in NSCP 2015. The frames will also be designed to withstand the minimum load requirements in NSCP 2015 and the seismic force obtained using the design response spectrum specified in Section 11.4.5 of ASCE 7-05 with the seismic hazard that corresponds to a 2% probability of recurring in 50 yr obtained from the PSHA results. The minimum base shear value was also calculated using Section 12.8.1 of ASCE 7-05 if the dynamic base shear was less than the static base shear and scaling will be required.

The ultimate load combinations used in the design of building samples were based on the NSCP 2015 with orthogonal application, as shown in Appendix V. On the other hand, the vertical and horizontal seismic loads were calculated using Equations 1 and 2 (based on ASCE 7-05 Section 12.4.2), where $E_h$ and $E_v$ are the horizontal and vertical earthquake forces, ρ is the redundancy factor, $S_{DS}$ is the design spectral acceleration at a short period earthquake, and DL is the seismic dead load of the structure. The redundancy factor was set to 1.0 for simplicity.

$$E_h = \rho Q_E \quad (1)$$

$$E_v = 0.2 S_{DS}\, DL \quad (2)$$

The entire design process of the building samples was carried out using ETABS, which is a software program capable of analyzing and designing the structural components of buildings following the set code requirements.

**Nonlinear Static Analysis**

One of the required inputs in the fragility analysis is the building's pushover curve; therefore, nonlinear pushover analysis was performed. The 12 designed building samples were re-modeled in SeismoStruct to perform nonlinear pushover analysis. SeismoStruct is a computer software suited for this study, as this can predict large displacement behaviors of frames under static or dynamic loading. This software is also capable of incorporating the geometric nonlinearities and material inelasticity of the structure in the analysis. The pushover curves resulting from each building sample were recorded. In addition, the fundamental period of each building sample was also recorded.

**Ground Motion Record Selection**

Another important input to conduct the fragility analysis of the building samples is the ground motion records. In this study, 11 strong ground motion acceleration time history records were selected. This was based on the minimum number of ground motion records required to conduct nonlinear response spectrum analysis based on

ASCE 7-16 Section 16.2.2, as there is no recommended minimum number of ground motion records to conduct fragility analysis. The selected ground motion records were obtained from seismic sources with similar characteristics to the West Valley Fault (WVF) using the Pacific Earthquake Engineering Research NGA-West2 strong ground motion database. The fault type used in the search was Strike-Slip since WVF is a dextral strike-slip fault (Rimando and Knuepfer 2006). The minimum and maximum magnitude inputs were based on source type A in NSCP 2015 (magnitude 7.0–8.4). The minimum and maximum input values for the closest distance to the surface projection of coseismic rupture, $R_{JB}$, were based on the source-to-site distance of the nearest and farthest grid points to the WVF. On the other hand, the minimum and maximum $V_{S30}$ values were based on Soil Type E ($V_{S30}$ = 180 m/s) and Soil Type A ($V_{S30}$ = 1500 m/s). The list of the selected ground motion records is shown in Appendix VI.

**Generic Fragility Curve Function**

FRACAS was used to obtain the fragility curve functions for each of the 12 building samples. FRACAS is a program created based on the study of Rossetto and co-authors (2016) which uses the pushover curve of the building and ground motion records to generate the building's fragility curve. There are different combinations of settings that can be chosen in FRACAS. The following settings used in this study are discussed in this section.

The damage index is used to quantify the amount of damage a structural member will have due to the applied ground motion. In FRACAS, the damage index of Rossetto and Elnashai (2003) was used considering inter-story drift ratios. The reason for utilizing the aforementioned damage index is two-fold – to maintain consistency with the program developers and to ensure its suitability for use in RC structures, following the analytical displacement-based procedure in the paper of Rossetto and Elnashai (2005). Ordinal regression was chosen as the fragility derivation method in FRACAS. The ordinal regression method is the same as the generalized linear model, wherein the engineered demand parameter (EDP) will be transformed into variables. The distribution of the variables with respect to the intensity measure (IM) will be used as parameters for the chosen link function to generate the fragility curve. The only difference between the ordinal regression method and the general linear model is that the ordinal regression method has additional constraints considering that the different damage states must be hierarchically ordered. This consideration will prevent the fragility curves from overlapping. With regards to the EDP and IM, maximum inter-story drift was chosen as the EDP, whereas $S_a$ was chosen as the IM.

The "probit" link function was used in the study, where it uses Equation 3 to derive the final fragility curve function shown in Equation 4, where $P_R$ is the probability of reaching the damage limit state, α is the mean (α = –a/b), β is the standard lognormal standard deviation (β = 1/b), Φ is the standard normal cumulative distribution function, whereas a and b are parameters calculated from the fragility derivation method.

$$\Phi^{-1}(P_R) = a + b \ln(S_a) \quad (3)$$

$$P_R = \Phi [(\ln(S_a) - \alpha) / \beta] \quad (4)$$

To establish the generic fragility function, the value of β must be obtained. The lognormal standard deviation value of each building sample is shown in Appendix VII. The value for β to be used in the generic fragility function was calculated by getting the average β value of the building samples which was found to be 0.70. Luco and co-authors (2007) suggested that β = 0.80 which was estimated from the results of the ATC-63 project titled "Quantification of Building System Performance and Response Parameters," whereas ASCE 7-10 to the latest ASCE 7-16 recommends that β = 0.60. Silva and co-authors (2016), Vacareanu and co-authors (2018), and Taherian and Kalantari (2019) also utilized β = 0.6 for the RTGM maps in their respective countries. Douglas and co-authors (2013) find that using a high β value (*e.g.* greater than 0.8) is very unlikely and produces unrealistic results. They also estimated the β is equal to 0.5 for France. Kharazian and co-authors (2021) utilized β = 0.7 for the RTGM map of Spain. A β value equal to 0.7 was also adopted in developing the RTGM map in SNI-1726-2012 in Indonesia but has been reduced to 0.65 based on the consensus of experts (Sengara *et al.* 2020). Based on previous studies, the researchers deemed that the β value ranges from 0.6–0.8, and the estimated β = 0.7 is reasonable to be used for this study. As part of this inquiry, a sensitivity analysis was conducted to know how the β value affects the $MCE_R$ spectral acceleration values by using the obtained average β (0.70) with β = 0.60 and 0.80, which will be discussed in the succeeding sections.

The generic fragility function will take the form of Equation 5 with β = 0.70. α is to be calculated using Equation 5 by setting the collapse probability at MCE, $P_R$, equal to 10%, as suggested in ASCE 7-16 Section 21.2.1.2 Method 2. $S_{aR}$ in Equation 5 is the spectral acceleration describing the $MCE_R$.

$$P_R = \Phi [(\ln(S_{aR}) - \alpha) / \beta] \quad (5)$$

**Probabilistic Risk-targeted Maximum Considered Earthquake ($MCE_R$)**

A risk target needs to be established to obtain the probabilistic $MCE_R$. Luco and co-authors (2007) created the RTGM maps of the US by using a risk target of a 1% probability of collapse in 50 yr based on the estimated

mean annual frequency of collapse to buildings designed using the American codes and standards during an MCE event. The studies of Goulet and co-authors (2007) and Fajfar and Dolsek (2012) yield similar collapse probabilities of code-based designed structures despite using different approaches. Vacareanu and co-authors (2018), Sengara and co-authors (2020), and Taherian and Kalantari (2019) used the same risk target in their studies and RTGM maps. Douglas and co-author (2013) deemed that a 1% probability of collapse in 50 yr ($2.0 \times 10^{-4}$) is too high to be applied to the RTGM maps of France and, therefore, utilized a risk target of collapse of $1.0 \times 10^{-5}$, which was also been used by Kharazian and co-authors (2021) in Spain. On the other hand, Silva and co-authors (2016) used an approximate but relatively higher annual probability of collapse ($5.0 \times 10^{-5}$) for Europe. Since NSCP 2015 reinforced concrete (RC) design procedures were based on American Concrete Institute's ACI 318 standard and the minimum load requirements were based on the American Society of Civil Engineers' ASCE 7-05 standard (ASEP 2015), the researchers assumed that the RC buildings in the Philippines will approximately have the same average mean annual frequency of collapse used by Luco and co-authors (2007). Thus, the uniform risk target used in this study, to calculate the probabilistic $MCE_R$, is 1% probability of collapse in 50 yr.

After the preparatory work of obtaining the generic fragility curve function and calculating the probabilistic seismic hazard curves, the probabilistic $MCE_R$ was determined by following the iterative process shown in Appendix VIII, as suggested by Luco and co-authors (2007). The probabilistic $MCE_R$ will be described by the calculated spectral acceleration values. This process was done for periods 0.2 and 1.0 s for every soil profile type ($S_A$–$S_E$).

**Deterministic Seismic Hazard Assessment (DSHA)**

It is possible that the calculated probabilistic $MCE_R$ spectral acceleration is greater than the spectral acceleration from the maximum ground motion of the nearby seismic source. It is not reasonable to consider high spectral acceleration values that are impossible to occur; thus, maximum spectral acceleration values were established. DSHA was performed to determine the maximum ground motion spectral acceleration values that the governing seismic source can produce.

DSHA was conducted using the next-generation attenuation (NGA) model of Boore and Atkinson (2008), which will be denoted as BA08, as the predictive equation to generate the 5% damped pseudo-absolute acceleration response spectrum. BA08 was chosen based on the applicability and availability of data. In addition, the 2008 version of Boore and Atkinson's NGA model was chosen instead of the updated 2014 version to maintain consistency with the GMPE version used by Peñarubia and co-authors (2020) and Allen and co-authors (2014) in conducting PSHA. BA08 is one of the five NGA models developed for shallow crustal earthquakes in the western United States – together with Abrahamson *et al.* (2008). According to Campbell and Bozorgnia (2006) and Stafford and co-authors (2008), the previously mentioned NGA models are suggested to be globally applicable for shallow crustal earthquakes in active regions based on their studies. Also, Abrahamson and co-authors' (2008) NGA comparison shows that the results of the five NGA models show similar median values for vertical strike-slip faults with magnitude ranges from 5.5–7.5, and standard deviation values are similar for magnitudes greater than 6.5.

The WVF was determined to be the major earthquake source for the City of Manila, its characteristics were obtained from the Greater Metro Manila area earthquake risk analysis Report by Allen and co-authors (2014). According to the report, WVF is a strike-slip fault that can produce an earthquake with a conservative range of magnitudes 6.4–7.3 (Allen *et al.* 2014). In this study, magnitude 7.3 was used as the maximum magnitude earthquake that the WVF can produce. Additionally, the source-to-site distances of each grid point were obtained using Hazard Hunter PH (hazardhunter.georisk.gov.ph) using the grid points mentioned previously as site locations.

The average shear wave velocity of the upper 30 m of the soil layer, $V_{s30}$, input values are the same values used in PSHA, as shown in Appendix II. The 84$^{th}$ percentile of the DSHA response spectrum was taken as the deterministic ground motion based on ASCE 7-16 Section 21.2.2.

In the US, the structures that were designed using the seismic provisions of the Uniform Building Code (UBC 1994) found in coastal California performed satisfactorily in past earthquakes (BSSC 2004). Considering the performance of the structures and the criteria of the UBC, the ceiling earthquake values in this provision were deemed to be appropriate to be used with the provisions for the MCE ground motion maps (BSSC 2004). ASCE 7 uses the maximum earthquake values from UBC 1994 as the lower limit for the deterministic ground motion for MCE and $MCE_R$ (ASCE 7-05; ASCE 7-10; ASCE 7-16). In this study, the lower limit values specified in ASCE 7-16 – including the site coefficients in the said provision – were used. Appendix IX shows the site coefficient values $F_a$ and $F_v$ corresponding to spectral accelerations $S_S = 1.5$g and $S_1 = 0.6$g, whereas Figure 21.2-1 of ASCE 7-16 shows the Deterministic Lower Limit response spectrum. The final deterministic ground motion values will be greater between the results of the DSHA and the deterministic lower limit values.

### Risk-targeted Maximum Considered Earthquake ($MCE_R$)

The final $MCE_R$ spectral acceleration values were taken as the lesser of the spectral acceleration results from the probabilistic RTGM and deterministic ground motion. To consider the maximum direction of the ground motion acting on buildings, directivity factors were multiplied by the final RTGM spectral acceleration. Huang and co-authors (2008) suggested using directivity factors to estimate the earthquake maximum response. His study was also the basis of the use of the directivity factors discussed in the 2009 edition of the National Earthquake Hazards Reduction Program recommended seismic provisions (BSSC 2009). Huang and co-authors (2008) suggested that ground motions at a 0.20-s period will have a directivity factor of 1.1, whereas ground motions at a 1.0-s period will have a directivity factor of 1.3.

### Risk-targeted Hazard Maps ($MCE_R$ Map and Risk Coefficient Map)

Two types of maps were developed in this study: [1] $MCE_R$ maps that can be used directly to calculate the seismic forces for the design of buildings, and [2] risk-coefficient ($C_R$) maps that can be used to convert the MCE site-specific ground motion to probabilistic $MCE_R$. The $MCE_R$ maps are the compilation of the calculated $MCE_R$ spectral acceleration values, whereas the $C_R$ maps will be the compilation of the ratio of the spectral acceleration values of the probabilistic $MCE_R$ and the MCE, as shown in Equation 6 (where T is the earthquake response period, $pMCE_R$ is the probabilistic $MCE_R$ spectral acceleration, and MCE is the maximum considered earthquake spectral acceleration obtained in PSHA).

$$C_{R,T} = pMCE_{R,T} / MCE_{,T} \quad (6)$$

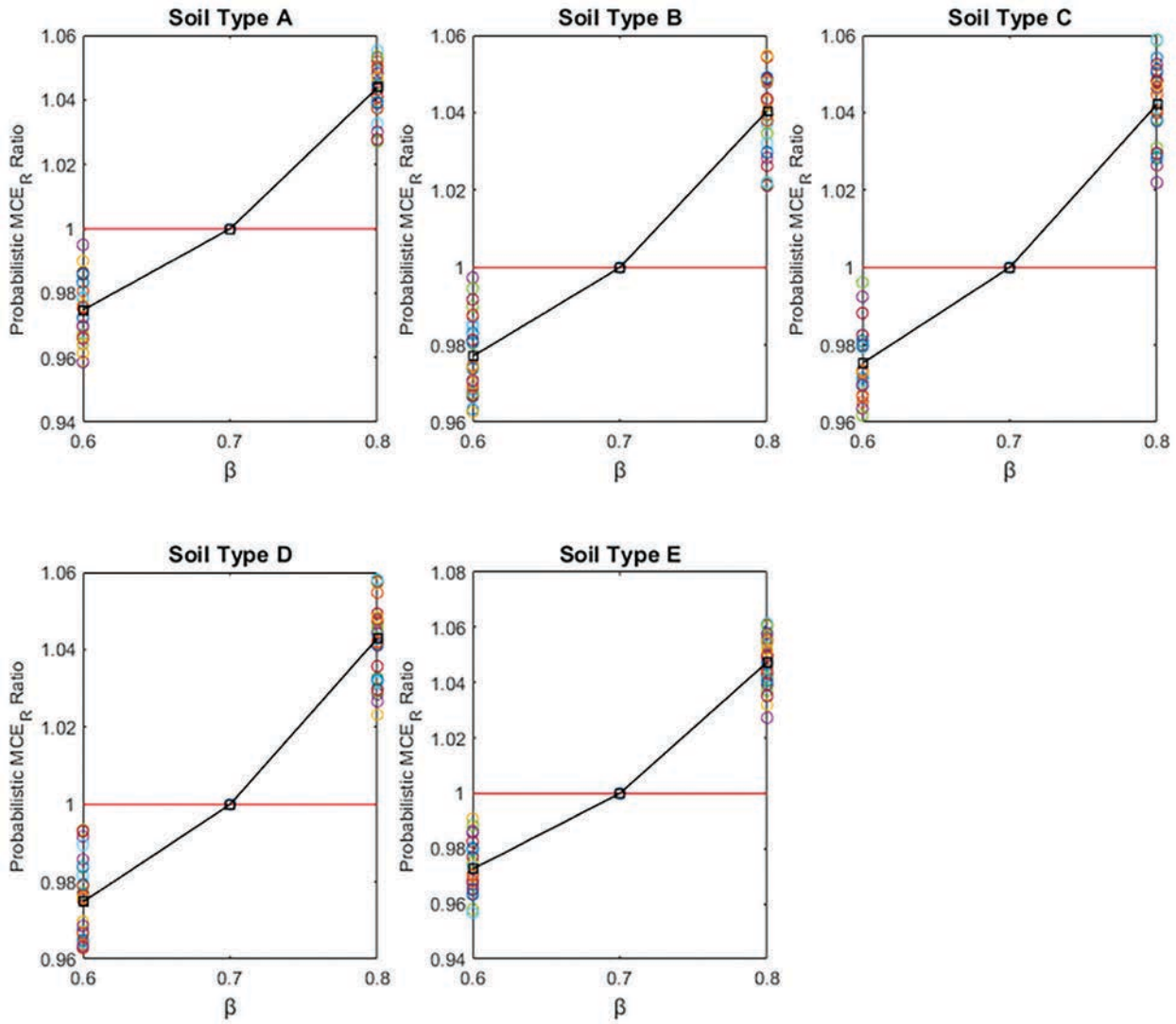


**Figure 1.** Probabilistic $MCE_R$ ratio using $\beta = 0.8$ and 0.6 with reference to $\beta = 0.7$.

The maps were plotted in spectral colors based on the values. For each type of map, two sets of maps were created for each soil type (a total of 10 maps for each type of map), which are maps for ground motions at T = 0.2 s and maps for ground motions at T = 1.0 s, where T is the ground motion response period. It is important to note that since the resulting spectral accelerations ($S_S$ and $S_1$) using the $C_R$ map are probabilistic $MCE_R$ spectral accelerations, the values must still be compared with the deterministic ground motion values. As mentioned in the previous sections, the lesser of the probabilistic and deterministic ground motion shall be considered as the RTGM that will be multiplied by the directivity factors.

## RESULTS AND DISCUSSION

A sensitivity study was conducted to investigate the correlation of the β to the probabilistic $MCE_R$. The probabilistic $MCE_R$ values were calculated using β = 0.60 and 0.80. The probabilistic $MCE_R$ values obtained were divided by the probabilistic $MCE_R$ when β = 0.70. The results are plotted as shown in Figure 1. The results show that β is directly proportional to the $MCE_R$. The results also show that the difference between the $MCE_R$ values when β = 0.70 against the $MCE_R$ values when β= 0.60 and 0.80 is approximately equal to or less than 5%.

The $C_R$ maps shown in Figures 2 and 3 show the ratio between the probabilistic $MCE_R$ and the MCE for different soil types. Looking at the $C_R$ map, the increase or decrease in spectral acceleration values due to the effects of incorporating the collapse capacity of buildings in the hazard can be easily seen. Ratios greater than 1.0 indicates that there is an increase in ground motion spectral acceleration and are represented in shades of red. On the contrary, ratios less than 1.0 indicates that there is a decrease in ground motion spectral acceleration and are represented in shades of blue. Considering soil types A and D for T = 0.20 s, some areas in Manila have increased ground motion but only ranging from 1–1.02 times. The whole area of Manila will likely have an increase in ground motion considering soil type E. Meanwhile, $C_R$ maps for T = 1.0 s show a decrease in spectral acceleration for all soil types. These results show how the structural capacity amplifies or reduces the uniform ground motion expected to occur.

The final $MCE_R$ maps are shown in Figures 4 and 5. Two (2) sets of maps were created – namely, $MCE_R$ maps for $S_S$ (see Figure 4) with spectral accelerations that range

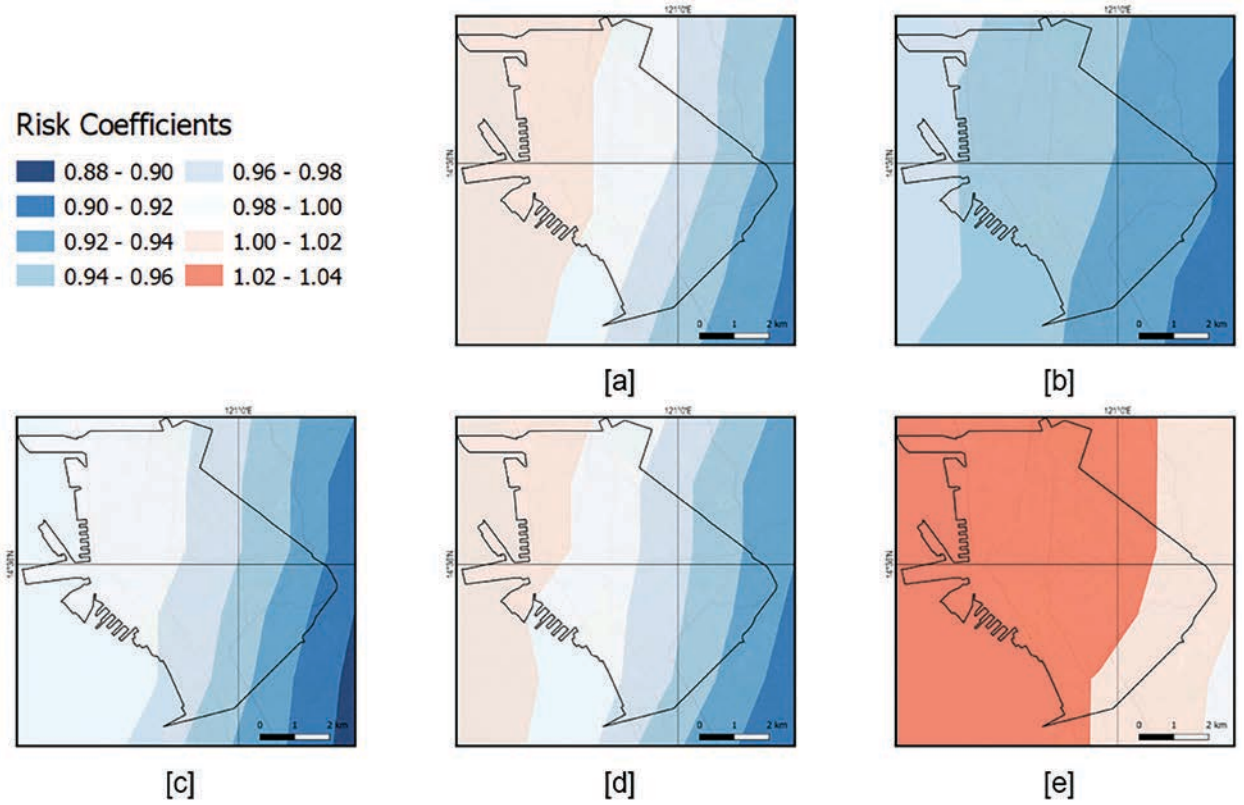


**Figure 2.** Risk coefficient maps at T = 0.2 s for [a] $S_A$, [b] soil profile type $S_B$, [c] soil profile type $S_C$, [d] soil profile type $S_D$, and [e] soil profile type $S_E$.

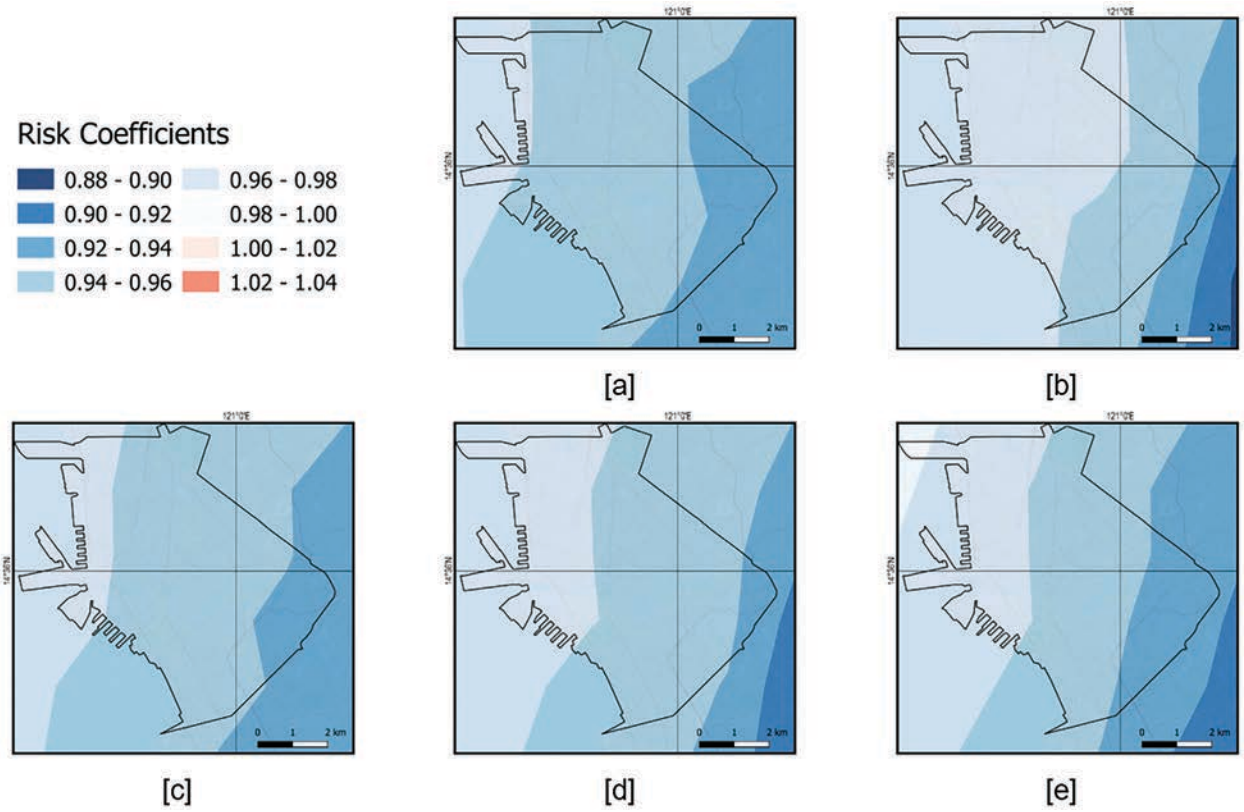


Figure 3. Risk coefficient maps at T = 1.0 s for [a] soil profile type $S_A$, [b] soil profile type $S_B$, [c] soil profile type $S_C$, [d] soil profile type $S_D$, and [e] soil profile type $S_E$.

from 1.03–1.25g, 1.25–1.55g, 1.74–1.98g, 1.65–1.70g, and 1.65g, for $S_A$, $S_B$, $S_C$, $S_D$, and $S_E$ soil profile types, respectively, and $MCE_R$ maps for $S_1$ (see Figure 5) with spectral accelerations that range from 0.49–0.60g, 0.57–0.65g, 0.83–1.05g, 0.91–1.20g, and 1.45–1.75g for the same profile types, respectively. Relative to the MCE values in SAM PH Atlas for the City of Manila ($S_s$ = 1.1–1.5g; $S_1$ = 0.41–0.60g), the $MCE_R$ values at soil profile $S_B$ in this study are generally slightly bigger, as influenced by the application of directivity factors.

## CONCLUSION AND RECOMMENDATION

The lognormal standard deviation, β, of the building samples considering Manila as the location, minimum design loads and requirements in NSCP 2015, and MCE design ground motion was found to be 0.70. This β value was used to define the generic fragility function representing the collapse capacity of the low-rise and mid-rise buildings in Manila. When the building fragility is integrated into the seismic hazard, it amplifies or reduces the ground motion spectral acceleration values. For the area of Manila, it is generally true that the probabilistic $MCE_R$ spectral accelerations are less than the MCE spectral accelerations. Although some areas may experience an increase in spectral acceleration values when T = 0.2 s, it is at most limited to a 4% increase. The $MCE_R$ maps that were developed in this study will provide information on MCE ground motions that will cause a uniform risk of collapse to buildings of 1% probability in 50 yr. The procedures done in this study may be replicated to create the $MCE_R$ maps in other areas of the country.

For the improvement of this study, the researchers recommend increasing the number of building samples and considering other building typologies to update the generic fragility function. The accuracy of the results in this study can further be improved if building inventory data are available. It is also recommended to investigate how the number of ground motions affects the lognormal standard deviation of the fragility of the building samples. Lastly, it is highly recommended to extend and expand the study's scope to other highly urbanized cities and the entire country.

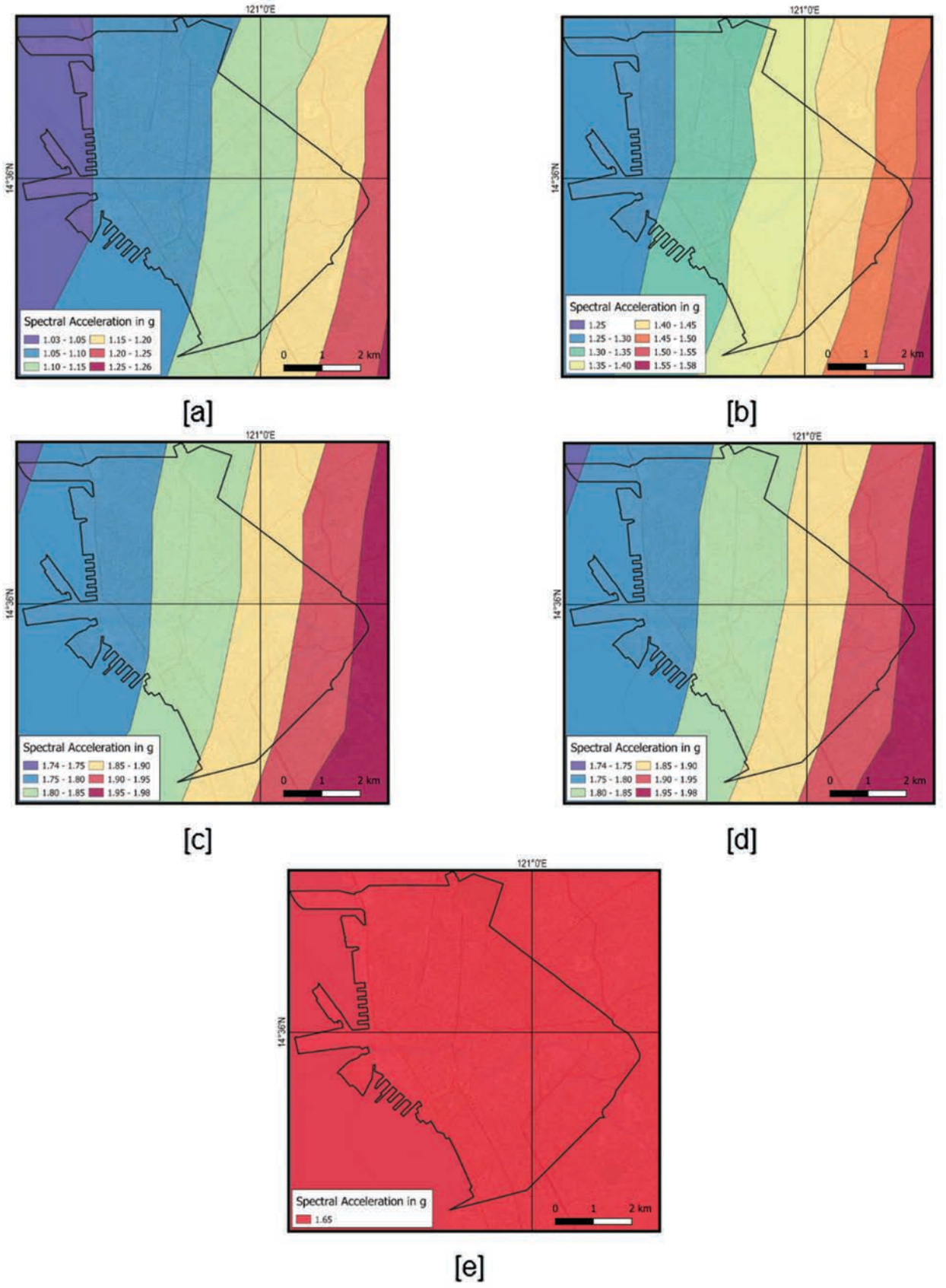


**Figure 4.** $MCE_R$ spectral response acceleration map of Manila for $S_S$ (T = 0.2 s) on soil profile type: [a] $S_A$, [b] $S_B$, [c] $S_C$, [d] $S_D$, and [e] $S_E$.

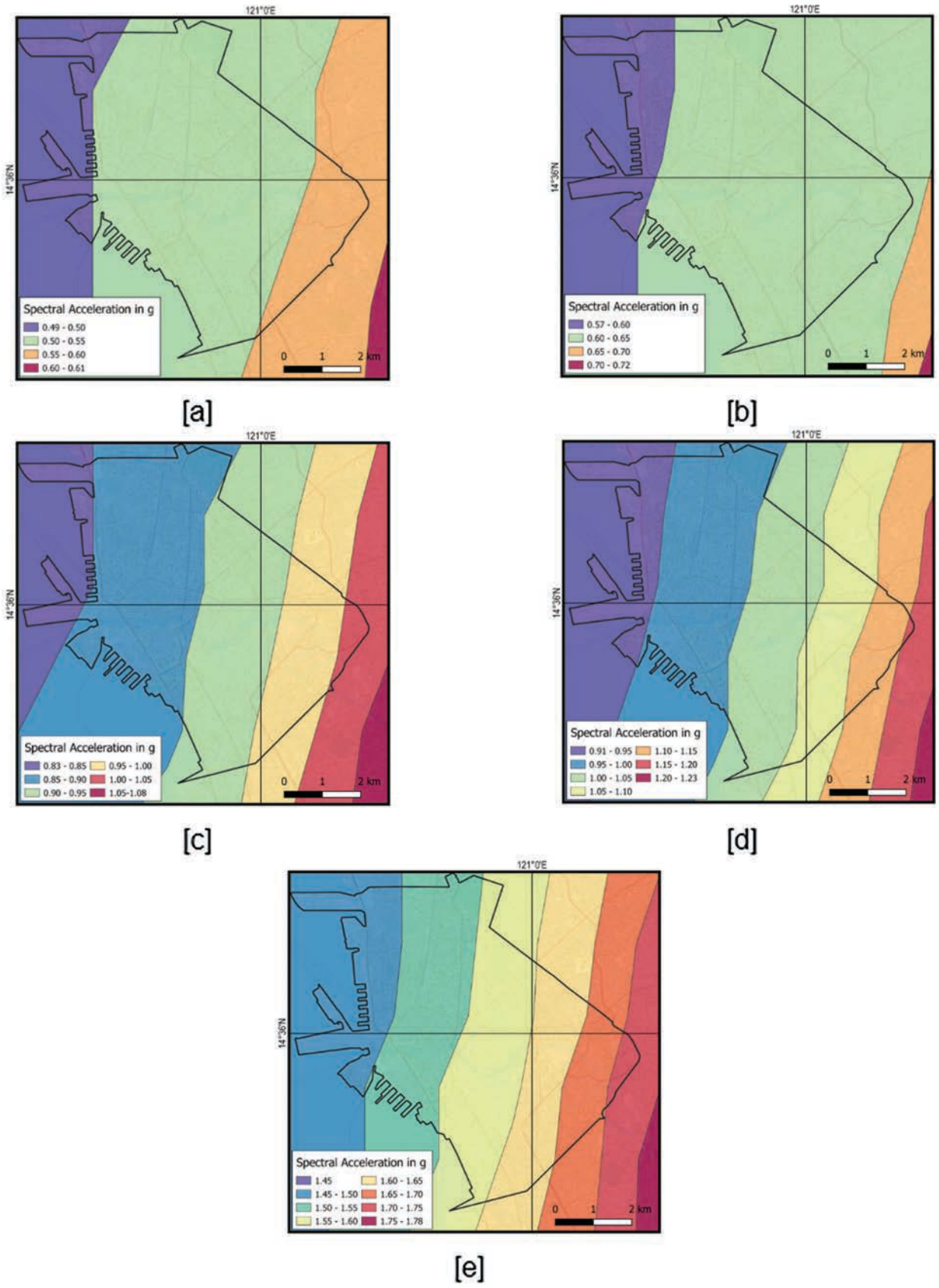


**Figure 5.** $MCE_R$ spectral response acceleration map of Manila for $S_1$ (T = 1.0 s) on soil profile type: [a] $S_A$, [b] $S_B$, [c] $S_C$, [d] $S_D$, and [e] $S_E$.

## ACKNOWLEDGMENT

The researchers would like to acknowledge and thank their beloved families, friends, and colleagues for their inspiration and support throughout this study. They would also like to acknowledge Engr. Randy B. Salazar for his valuable input and support. Finally, the researchers would like to acknowledge the DOST-ERDT (Department of Science and Technology–Engineering Research and Development Technology) for the financial support extended to the first author.

## NOTE ON APPENDICES

The complete appendices section of the study is accessible at https://philjournsci.dost.gov.ph.

## STATEMENT ON CONFLICT OF INTEREST

No conflict of interest to declare.

## REFERENCES

ABRAHAMSON N, ATKINSON G, BOORE D, BOZORGNIA Y, CAMPBELL K, CHIOU B, IDRISS IM, SILVA W, YOUNGS R. 2008. Comparisons of the NGA ground-motion relations. Earthquake Spectra 24(1): 45–66.

ALLEN T, RYU H, BAUTISTA B, LEONILA BAUTISTA M, NARAG I, SEVILLA WI, LYN M, MELOSANTOS P, PAPIONA K, BONITA J. 2014. Enhancing risk analysis capacities for flood, tropical cyclone severe wind and earthquake for the Greater Metro Manila Area Component 5-Earthquake Risk Analysis. Retrieved on 07 Aug 2022 from https://ndrrmc.gov.ph/ attachments/ article/1509/Component_5_Earthquake_Risk_Analysis_Technical%20Report_-_Final_Draft_by_GA_and_PHIVOLCS.pdf

[ASCE] American Society of Civil Engineers. 2005. ASCE/SEI 7-05 Minimum Design Loads for Buildings and Other Structures. Reston, Virginia, United States.

[ASCE] American Society of Civil Engineers. 2017. ASCE/SEI 7-16 Minimum Design Loads and Associated Criteria for Buildings and Other Structures. Reston, Virginia, United States.

[ASEP] Association of Structural Engineers of the Philippines. 2015. National Structural Code of the Philippines 2015, Volume 1. Quezon City, Philippines.

BOORE DM, ATKINSON GM. 2008. Ground-motion prediction equations for the average horizontal component of PGA, PGV, and 5%-damped PSA at spectral periods between 0.01 s and 10.0 s. Earthquake Spectra 24(1): 99–138.

[BSSC] Building Seismic Safety Council. 2004. NEHRP recommended provisions for seismic regulations for new buildings and other structures (FEMA 450) part 2: commentary, 2003 ed. Federal Emergency Management Agency, Washington, District of Columbia, United States.

[BSSC] Building Seismic Safety Councill. 2009. NEHRP Recommended Seismic Provision for New Buildings and Other Structures (FEMA P-750). Federal Emergency Management Association, Washington, District of Columbia, United States.

CAMPBELL KW, BOZORGNIA Y. 2006. In: Next Generation Attenuation (NGA) Empirical Ground Motion Models: Can They be Used in Europe? Proceedings on the First European Conference on Earthquake Engineering and Seismology; 2006; Geneva, Switzerland. No. 458, p. 10.

[DOST-PHIVOLCS] Department of Science and Technology–Philippine Institute of Volcanology and Seismology. 2017. The Philippine Earthquake Model. Quezon City, Philippines. Retrieved on 24 Jan 2020 from http://www.phivolcs.dost.gov.ph

[DOST-PHIVOLCS] Department of Science and Technology–Philippine Institute of Volcanology and Seismology. 2021. Spectral Acceleration Maps of the Philippines (SAM PH). Quezon City, Philippines. Retrieved on 07 May 2021 from http://www.phivolcs.dost.gov.ph

DOUGLAS J, GKIMPRIXIS A, TUBALDI E. 2019. In: Derivation of Risk-targeted Maps for Italy Based on a Simplified Approach. Proceedings of the XVIII Convegno ANIDIS L'ingegneria Sismica in Italia: Ascoli Piceno; 2019; Pisa, Italy. p. 15–19.

DOUGLAS J, ULRICH T, NEGULESCU C. 2013. Risk-targeted seismic design maps for mainland France. Natural Hazards 65: 1999–2013.

FAJFAR P, DOLSEK M. 2012. A practice-oriented estimation of the failure probability of buildings. Earthquake Engineering and Structural Dynamics 41: 679–691.

GKIMPRIXIS A, TUBALDI E, DOUGLAS J. 2019. Comparison of methods to develop risk-targeted seismic design maps. Bulletin of Earthquake Engineering 17: 3727–3752.

GOULET CA, HASELTON CB, MITRANI-REISER J, BECK JL, DEIERLEIN GG, PORTER KA, STEWART JP. 2007. Evaluation of the seismic performance

of a code-conforming reinforced-concrete frame building – from seismic hazard to collapse safety and economic losses. Earthquake Engineering and Structural Dynamics 36: 1973–1997.

HUANG YN, WHITTAKER AS, LUCO N. 2008. Maximum spectral demands in the near-fault region. Earthquake Spectra 24(1): 319–341.

KHARAZIAN A, MOLINA S, GALIANA-MERINO JJ, AGEA-MEDINA N. 2021. Risk-targeted hazard maps for Spain. Bulletin of Earthquake Engineering 19: 5369–5389.

LUCO N, ELLINGWOOD BR, HAMBURGER RO, HOOPER JD, KIMBALL JK, KIRCHER CA. 2007. In: Risk-targeted *versus* current seismic design maps for the conterminous United States. Proceedings of a Convention on Structural Engineering Association of California; 2007; Structural Engineers Association of California, San Diego, California, United States. p. 1–13.

PEÑARUBIA HC, JOHNSON KL, STYRON RH, BACOLCOL TC, SEVILLA WIG, PEREZ JS, BONITA JD, NARAG IC, SOLIDUM RU, PAGANI MM, ALLEN TI. 2020. Probabilistic seismic hazard analysis model for the Philippines. Earthquake Spectra 36(1): 44–68.

RIMANDO RE, KNUEPFER, PLK. 2006. Neotectonics of the Marikina Valley fault system (MVFS) and tectonic framework of structures in northern and central Luzon, Philippines. Tectonophysics 415(1–4): 17–38.

ROSSETTO T, ELNASHAI A. 2003. Derivation of vulnerability functions for European-type RC structures based on observational data. Engineering Structures 25(10): 1241–1263.

ROSSETTO T, ELNASHAI A. 2005. A new analytical procedure for the derivation of displacement-based vulnerability curves for populations of RC structures. Engineering Structures 27: 397–409.

ROSSETTO T, GEHL P, MINAS S, GALASSO C, DUFFOUR P, DOUGLAS J, COOK O. 2016. FRACAS: a capacity spectrum approach for seismic fragility assessment including record-to-record variability. Engineering Structures 125: 337–348.

SILVA V, CROWLEY H, BAZZURRO P. 2016. Exploring risk-targeted hazard maps for Europe. Earthquake Spectra 32(2): 1165–1186

SENGARA W, IRSYAM M, SIDI ID, MULIA A, ASRURIFAK M, HUTABARAT D, PARTONO W. 2020. New 2019 risk-targeted ground motions for spectral design criteria in Indonesian seismic building code. E3S Web of Conference. 156p.

STAFFORD PJ, STRASSER FO, BOMMER JJ. 2008. An evaluation of the applicability of the NGA models to ground-motion prediction in the Euro-Mediterranean region. Bulletin of Earthquake Engineering 6(2): 149–177.

TAHERIAN AR, KALANTARI A. 2019. Risk-targeted seismic design maps for Iran. Journal of Seismology 23: 1299-1311.

VACAREANU R, PAVEL F, CRACIUN I, COLIBA V, ARION C, ALDEA A, NEAGU C. 2018. Risk-targeted maps for Romania. Journal of Seismology 22(2): 407–417.

# APPENDICES

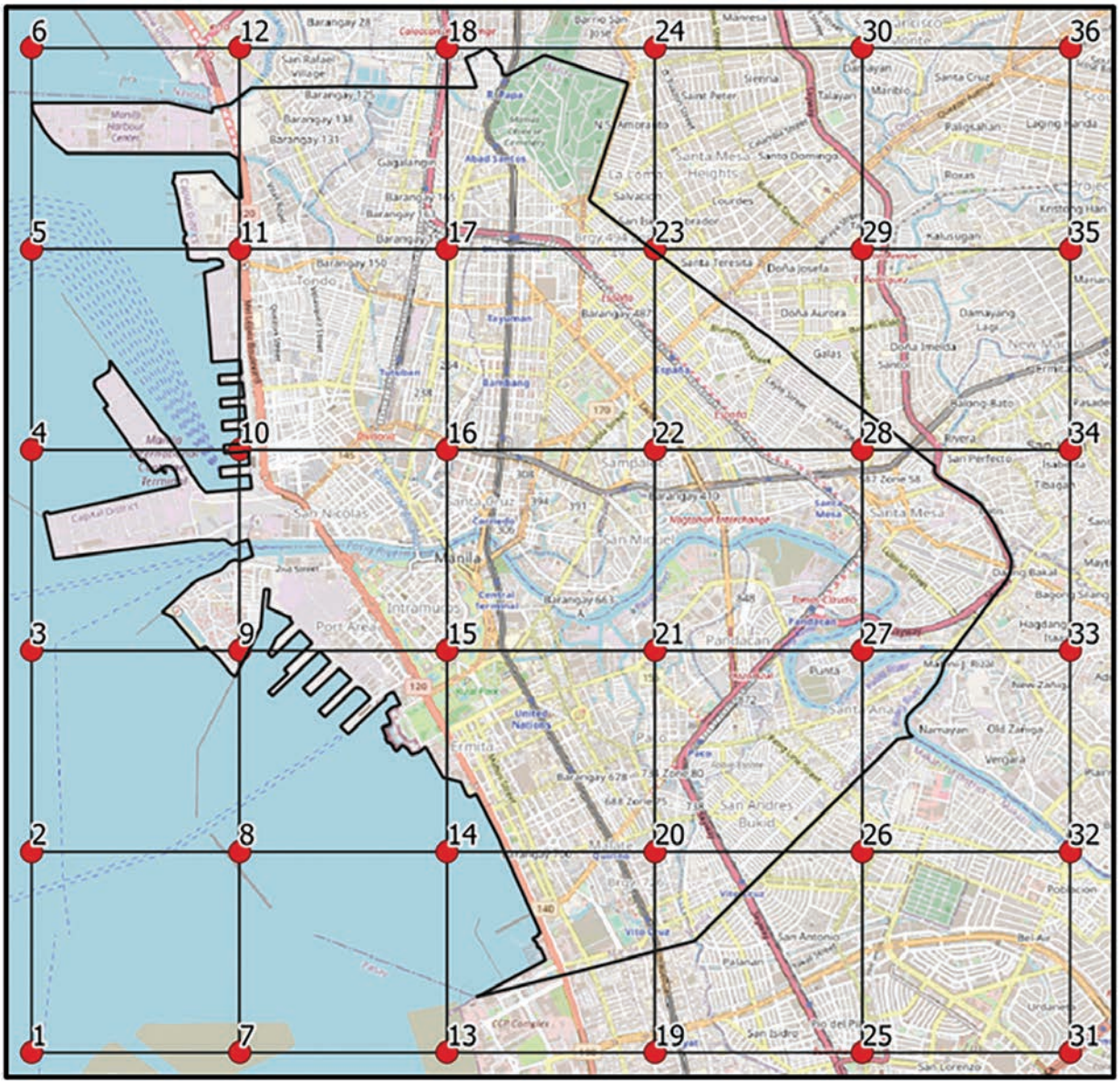


**Appendix I.** 2 km x 2 km grid layout for Manila, Philippines.

**Appendix II.** Shear wave velocity of different soil profile.

| Soil profile type | Generic description | Shear wave velocity, Vs (m/s) | Reference |
|---|---|---|---|
| $S_A$ | Hard rock | 1500 | NSCP 2015 |
| $S_B$ | Rock | 780 | SAM PH |
| $S_C$ | Very dense soil and soft rock | 560 | NSCP 2015 (mean value) |
| $S_D$ | Stiff Soil | 370 | NSCP 2015 (upper value) |
| $S_E$ | Soft Soil | 180 | NSCP 2015 |

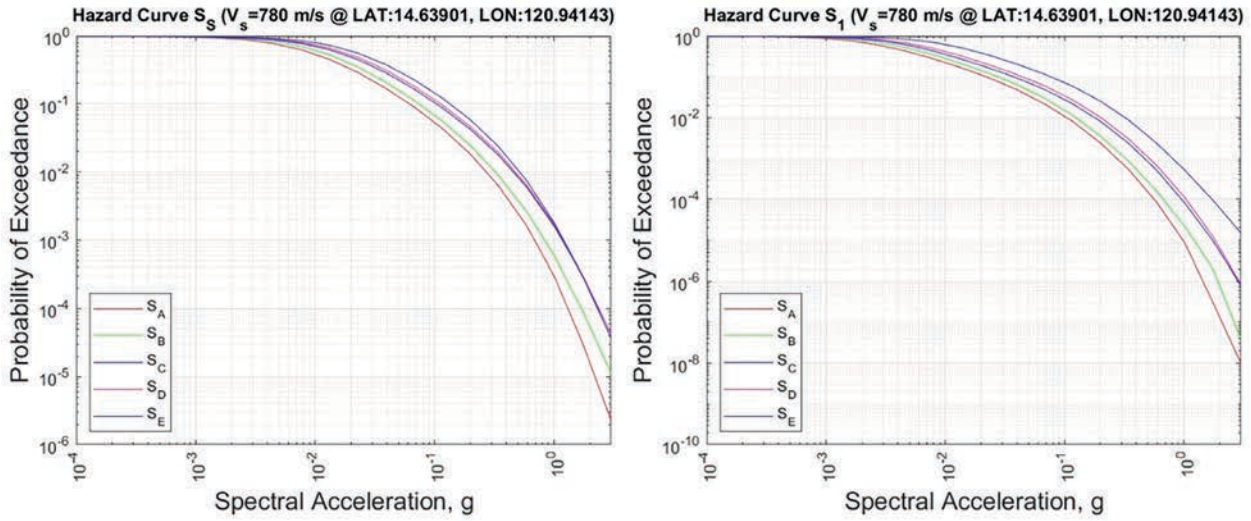


**Appendix III.** Seismic hazard curves $S_S$ (0.2 s spectral acceleration) and $S_1$ (1.0 s spectral acceleration) at latitude 14.63901, longitude 120.94143.

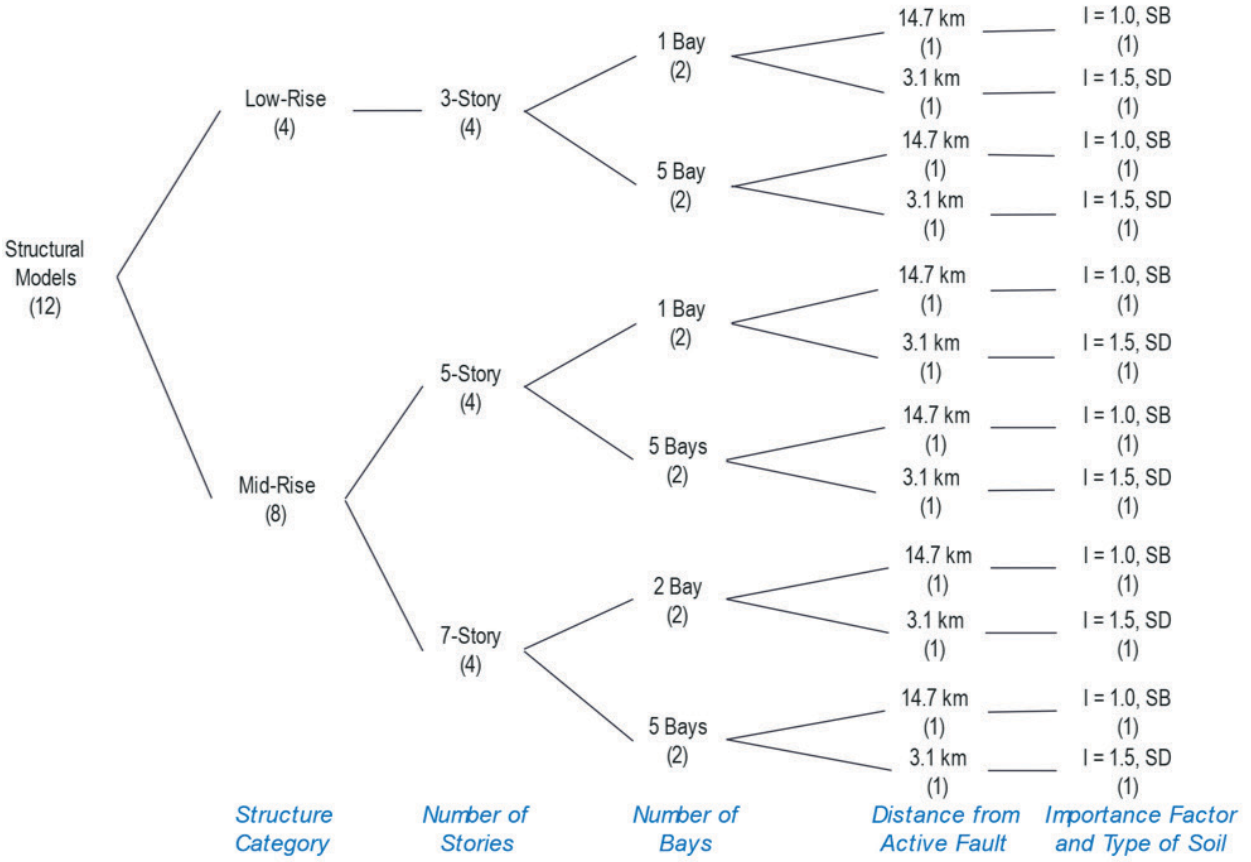


**Appendix IV.** Building sampling logic tree.

**Appendix V.** Ultimate load combinations based on the National Structural Code of the Philippines (NSCP 2015): [DL] dead load, [LL] live load, [$E_v$] vertical earthquake load, and [$E_{hx}$, $E_{hy}$] horizontal earthquake load at orthogonal directions.

| Load combinations |
|---|
| 1.40 DL |
| 1.20 DL + 1.60 LL |
| 1.20 DL + 0.50 LL + 1.00 $E_v$ + 1.00 $E_{hx}$ + 0.30 $E_{hy}$ |
| 1.20 DL + 0.50 LL + + 1.00 $E_v$ + 0.30 $E_{hx}$ + 1.00 $E_{hy}$ |
| 0.90 DL – 1.00 $E_v$ + 1.00 $E_{hx}$ + 0.30 $E_{hy}$ |
| 0.90 DL – 1.00 $E_v$ +0.30 $E_{hx}$ + 1.00 $E_{hy}$ |

**Appendix VI.** Selected earthquake time history records from PEER Ground Motion database.

| Record sequence number | Earthquake name | Station name | Distance from rupture, $R_{rup}$ (km) | Year | Magnitude |
|---|---|---|---|---|---|
| 864 | Landers | Joshua Tree | 11.03 | 1992 | 7.28 |
| 1165 | Kocaeli_Turkey | Izmit | 7.21 | 1999 | 7.51 |
| 1614 | Duzce_Turkey | Lamont 1061 | 11.46 | 1999 | 7.14 |
| 1615 | Duzce_Turkey | Lamont 1062 | 9.14 | 1999 | 7.14 |
| 1633 | Manjil_Iran | Abbar | 12.55 | 1990 | 7.37 |
| 5825 | El Mayor-Cucapah_Mexico | Cerro Prieto Geothermal | 10.92 | 2010 | 7.2 |
| 6893 | Darfield_New Zealand | DFHS | 11.86 | 2010 | 7.0 |
| 6897 | Darfield_New Zealand | DSLC | 8.46 | 2010 | 7.0 |
| 6930 | Darfield_New Zealand | LRSC | 12.52 | 2010 | 7.0 |
| 6975 | Darfield_New Zealand | TPLC | 6.11 | 2010 | 7.0 |
| 8606 | El Mayor-Cucapah_Mexico | Westside Elementary School | 11.44 | 2010 | 7.2 |

**Appendix VII.** Lognormal standard deviation for each building samples using XYZ-ABC format for the structure name: [X] building category, [Y] number of stories, [Z] number of bays, [A] location (either near or far to the WVF), [B] importance category based on NSCP 2015, and [C] soil profile type.

| Structure name | Lognormal standard deviation, β | Structure name | Lognormal standard deviation, β |
|---|---|---|---|
| L31-F3B | 0.59 | L31-N1D | 0.67 |
| L35-F3B | 0.68 | L35-N1D | 0.81 |
| M51-F3B | 0.78 | M51-N1D | 0.68 |
| M55-F3B | 0.75 | M55-N1D | 0.73 |
| M72-F3B | 0.73 | M72-N1D | 0.59 |
| M75-F3B | 0.76 | M75-N1D | 0.80 |

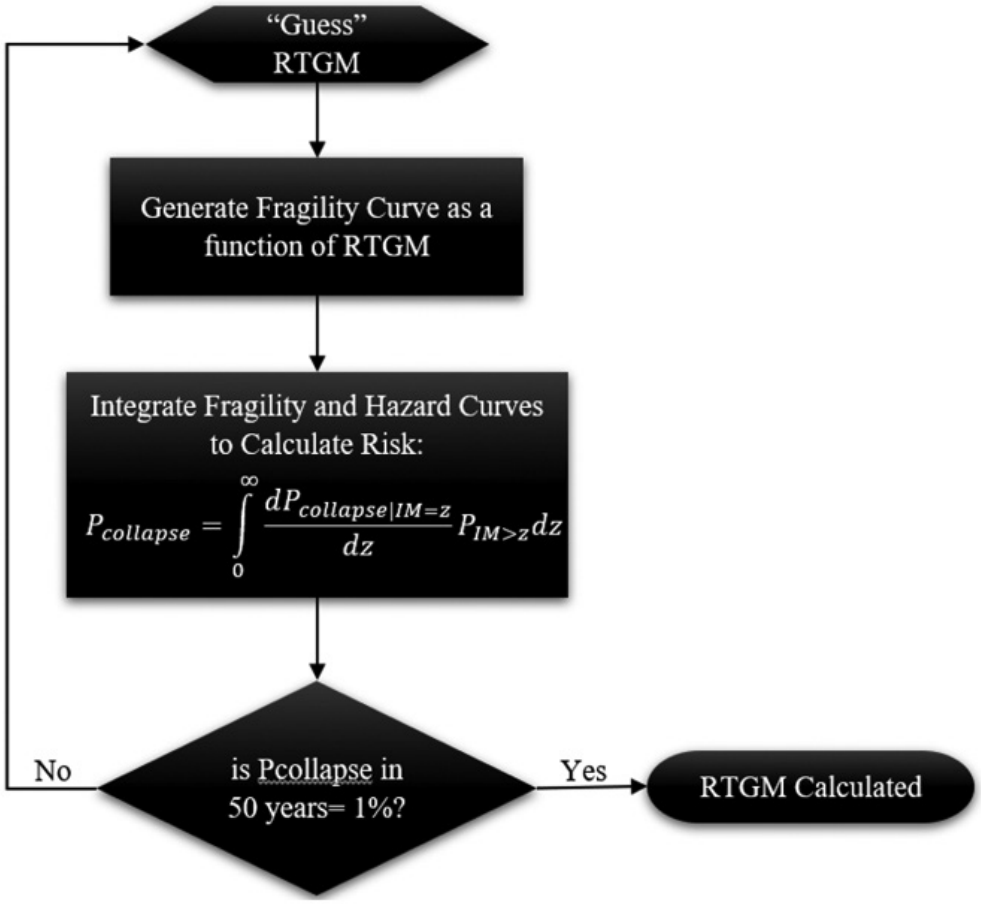


**Appendix VIII.** Probabilistic $MCE_R$ flowchart based on Luco and colleagues (2007).

**Appendix IX.** Site coefficient values at 0.2 s period ($F_a$) and 1.0 s period ($F_v$) according to ASCE/SEI 7-16 minimum loads and associated criteria for buildings and other structures

| Soil profile type | $F_a$ | $F_v$ |
|---|---|---|
| $S_A$ | 0.8 | 0.8 |
| $S_B$ | 0.9 | 0.8 |
| $S_C$ | 1.2 | 1.4 |
| $S_D$ | 1.0 | 2.5 |
| $S_E$ | 1.0 | 4.0 |